

# Development of Technology for Reduction of CO<sub>2</sub> Emission from Blast Furnace Using 12 m<sup>3</sup> Experimental Blast Furnace

Chikashi KAMIJO\*      Yoshinori MATSUKURA  
 Hirokazu YOKOYAMA      Kohei SUNAHARA  
 Kazumoto KAKIUCHI      Kaoru NAKANO  
 Hiroshi SAKAI

## Abstract

*The development of technology to reduce the amount of CO<sub>2</sub> emission from steelworks is a matter of urgency. In order to clarify the blast furnace process operation that maximizes the effect of hydrogen reduction, a technology for highly efficient use of hydrogen for iron ore reduction has been developed using a 12 m<sup>3</sup> experimental blast furnace in COURSE50. Operation tests were conducted for 32 days each in the 3Q of 2018 and the 1Q of 2019 to investigate the effect of blowing reduced gas containing hydrogen into the blast furnace on the amount of CO<sub>2</sub> emitted from the blast furnace. In addition, a three-dimensional blast furnace mathematical model was used to predict and calculate the amount of CO<sub>2</sub> emission and was reflected in the operational design of the test blast furnace. As a result, reducing CO<sub>2</sub> emissions by 10% has been achieved, which is the development target. Also, it was confirmed that the prediction accuracy of the model was extremely high.*

## 1. Introduction

On November 4, 2016, the Paris Agreement<sup>1)</sup> came into force as a new international framework to reduce greenhouse gas emissions after 2020. The development of technologies for reducing CO<sub>2</sub> emissions from steelworks is an urgent issue. Various technologies have been developed to protect the global environment.<sup>2)</sup> For example, the experimental operation by ThyssenKrupp using an actual blast furnace, in which pure hydrogen is injected from one of the tuyeres, has been conducted since 2019.<sup>3)</sup> Also, the pure oxygen injection test operation was conducted using a 430 m<sup>3</sup> experimental blast furnace that was modified from an actual furnace in July 2019 by the Baosteel Group Xinjiang Bayi Iron & Steel Co., Ltd. In addition, pure hydrogen injection tests are planned.<sup>4)</sup> In Japan, the development of oxygen blast furnaces has been ongoing.<sup>5,6)</sup> In a project titled “Development of Environmentally Friendly Process Technology” commissioned by the New Energy and Industrial Technology Development Organization (NEDO),<sup>7)</sup> Nippon Steel Corporation has been developing the technology for using ferrocoke<sup>8)</sup> and the technology for using hydrogen with high efficiency in iron ore reduction to clearly identify the blast furnace process operation that

can fully exploit the benefits of hydrogen reduction. The latter technology is called the CO<sub>2</sub> Ultimate Reduction System for Cool Earth 50 (COURSE50).

From fiscal 2018, the tuyere injection of hydrogen-based gaseous reductant at a maximum rate of 277 Nm<sup>3</sup>/t-HM was simulated and the variation in the volume of CO<sub>2</sub> emission was analyzed using a three-dimensional mathematical blast furnace model<sup>9,10)</sup> in COURSE50. This simulation was conducted to prepare for the tuyere injection of a large volume of hydrogen-based gaseous reductant. The simulation results were reflected in the operational design of an experimental blast furnace. The experimental operations, each of which lasted for 32 days, were conducted in the third quarter of fiscal 2018 and the first quarter of fiscal 2019, and the effects of blast furnace injection of hydrogen-containing gaseous reductant on CO<sub>2</sub> emissions from the blast furnace were investigated.

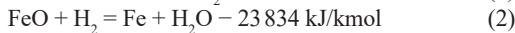
## 2. Development Outline of COURSE50

COURSE50 is a project designed to reduce the CO<sub>2</sub> emissions from steelworks by 30% by taking full advantage of existing steelworks' equipment. Of the 30% CO<sub>2</sub> emission reduction, 20%

\* Chief Manager, Ph.D. (Engineering), Experimental Blast Furnace Project Div., Process Research Laboratories  
 1 Kimitsu, Kimitsu City, Chiba Pref. 299-1141

achievement by separation and recovery of CO<sub>2</sub> in the top gas of the blast furnace and 10% achievement by the blast and raw material operation of the blast furnace are planned. In fiscal 2008, the 100% NEDO-subsidized COURSE50 project was launched by the following six companies: Nippon Steel Corporation, Sumitomo Metal Industries Ltd., Nisshin Steel Co., Ltd., JFE Steel Corporation, Kobe Steel, Ltd., and Nippon Steel Engineering Co., Ltd. (The first three companies are now under the umbrella of the current Nippon Steel). The elementary technology development was carried out up to fiscal 2012 (Phase I-STEP 1). Then the development of a comprehensive technology integrating hydrogen reduction and CO<sub>2</sub> separation and recovery, mainly using the experimental blast furnace was conducted from fiscal 2013 to fiscal 2017 (Phase I-STEP 2).<sup>11-13)</sup>

A conventional blast furnace and the COURSE50 blast furnace are comparatively illustrated in Fig. 1. Of the reduction reactions taking place in the conventional blast furnace, 60% are accounted for by CO gas reduction, 10% by H<sub>2</sub> gas reduction, and 30% by direct reduction in which FeO is reduced by apparently solid C. The equations and heats of these reactions are given by



The COURSE50 blast furnace aims to replace 10% of direct reduction with the H<sub>2</sub> gas by injecting hydrogen-based gaseous reductant. Although the direct reduction and the H<sub>2</sub> reduction are both endothermic reactions, replacement of the direct reduction with the H<sub>2</sub> reduction can reduce both the reducing agent ratio and the CO<sub>2</sub> emissions because the heat absorption of the direct reduction is much larger.

To verify this concept, a three-dimensional mathematical blast furnace model<sup>10)</sup> adapted for the high hydrogen injection operation described later was developed and simulations were performed using it. In 2016, an experimental blast furnace with an inner volume of 12 m<sup>3</sup> was constructed, and two hot test runs and four operation trials were conducted to verify the simulation results. Consequently, the initial target of 10% CO<sub>2</sub> emissions reduction was achieved by employing the following three processes: (1) injection of coke oven gas (COG) through the tuyeres and high oxygen enrichment of blast air, (2) shaft tuyere injection of the gas left after the separation of CO<sub>2</sub> from the top gas, and (3) use of high reducibility sinter (Fig.

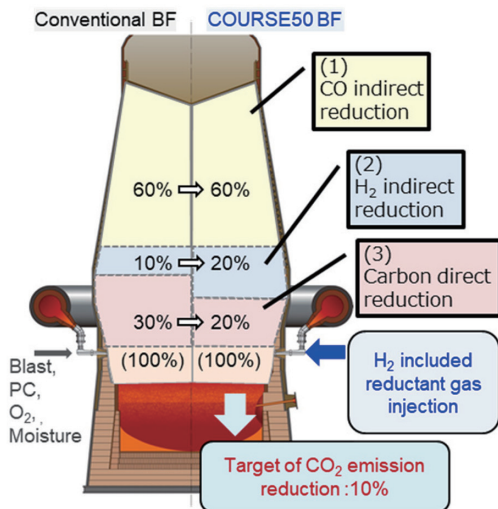


Fig. 1 Comparison of conventional BF with COURSE50 BF

2 a)).

To expand the freedom of the processes for reducing CO<sub>2</sub> emissions, the development seeking the upper limit of the CO<sub>2</sub> emissions reduction was started in fiscal 2018 (Phase II-STEP 1) by the following two processes: (1) tuyere injection of hydrogen-based gaseous reductant and high oxygen enrichment of blast air, and (2) use of high reducibility sinter (Fig. 2b)).

### 3. Equipment Outline of Experimental Blast Furnace

The 12 m<sup>3</sup> experimental blast furnace is schematically illustrated in Fig. 3.<sup>12)</sup> This is a bell-less type blast furnace with one tap hole and three tuyeres. Hot blast at about temperature of 1000°C from hot stoves is blown into the experimental blast furnace to produce pig iron. Pulverized coal and hydrogen-containing gaseous reductant are injected into the tuyeres through double-tube or triple-tube lances. As with an actual blast furnace, sinter and lump ore, slag composition adjusting flux, and lump coke are drawn from raw material hoppers, carried by conveyor belts to the furnace top, and charged layer by layer into the blast furnace. When the blast furnace

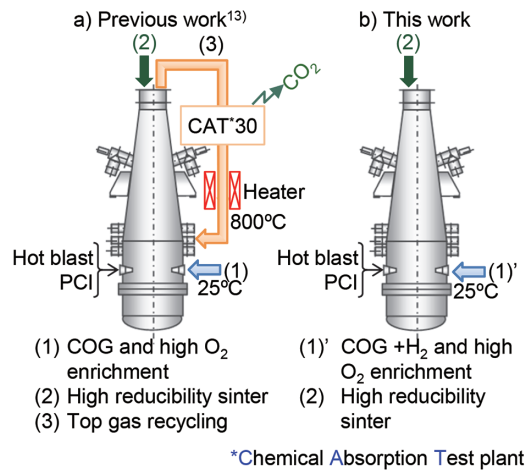


Fig. 2 Comparison of schematic views of operation configurations

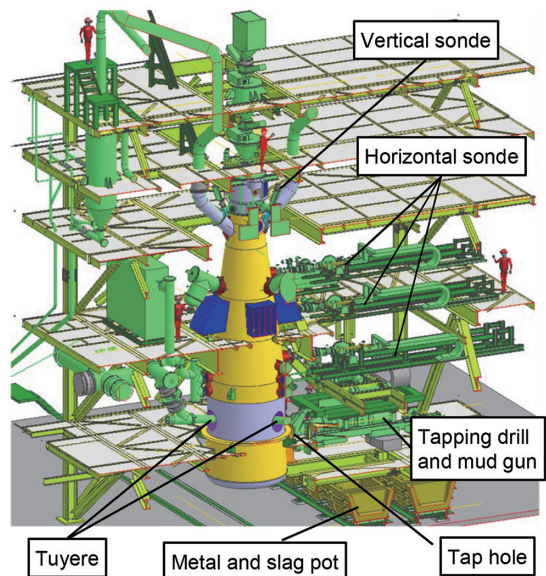


Fig. 3 Schematic view of 12 m<sup>3</sup> experimental blast furnace<sup>12)</sup>

operation conditions are designed to achieve a pig iron production rate of 34 tons per day, the tap hole is opened with a tap hole drill every 2 hours. About 4 tons of pig iron and slag are discharged in one tapping and received into a metal and slag pot. The experimental blast furnace is equipped with all of the measuring sensors installed on conventional blast furnaces, such as vertical probes, temperature measuring thermocouples, and static pressure gauges. As measuring sensors are not installed on conventional blast furnaces, the test blast furnace is fitted with probes in three stages in the vertical direction for sampling burden materials and furnace gases.

#### 4. Experimental Procedures

##### 4.1 Outline and simulation conditions of three-dimensional mathematical blast furnace model

###### 4.1.1 Outline

The three-dimensional mathematical blast furnace model<sup>9,10)</sup> is schematically illustrated in Fig. 4. The hearth is excluded from the calculation domain. Material, energy, and momentum balance equations related to gas, solid, and liquid phases are considered. The main reactions considered in the model are listed in Table 1. Equations (4) to (9) are concerned with the reduction of iron oxide and are calculated using a three-interface unreacted core model. Equations (10) and (11) are the gasification reactions of coke. These reaction rates are calculated using Arrhenius type chemical reaction rate constants derived from the previous fundamental studies. The rate constants can be multiplied by correction factors. When simulating the operation of the experimental blast furnace, the values of the correction factors are determined from the performance analysis results of the furnace. The prediction accuracy is improved by using the correction factors.

###### 4.1.2 Simulations

To investigate the influence of the hydrogen containing gas injection rate on the effect of CO<sub>2</sub> emission reduction, the operation of the experimental blast furnace with the injection of COG alone, both COG and H<sub>2</sub>, and H<sub>2</sub> alone was simulated.

##### 4.2 Operation of experimental blast furnace

###### 4.2.1 Operation conditions

Table 2 shows the operation conditions designed by the three-dimensional mathematical blast furnace model for the fifth and sixth campaigns and the specific carbon consumption reduction ratio predicted by the model for those campaigns. The operation conditions of the experimental blast furnace were designed to keep constant the flame temperature, pig iron temperature, and pig iron production rate. Case A is the conventional actual blast furnace operation condition. This operation was constantly conducted to check that the respective operation tests did not deviate from the standard conditions due to disturbances. Two cases in the sixth campaign were appended with “-2” to distinguish them from the corresponding cases in the fifth campaign. Case C was conducted in both the fifth and sixth campaigns to check the operation reproducibility with a high hydrogen injection rate. The test values are somewhat different between Case C in the fifth campaign and Case C-2 in the sixth campaign. These are the results of the re-tuning conducted after the fifth campaign as described later. The total hydrogen input rate was practically the same between Cases B and E and among Cases C, C-2, and F. The type of gas injected through the tuyeres was changed in those cases. In addition, the total hydrogen input rate means the sum total of the hydrogen derived from COG and/or pure H<sub>2</sub> gas injected through the tuyeres, and derived from the pulverized coal and coke burnt in front of the tuyeres. Although the operation conditions in

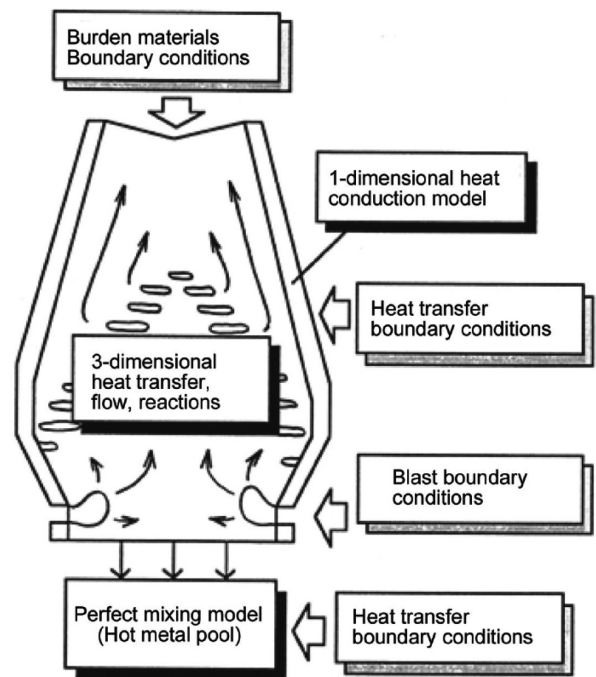


Fig. 4 Schematic diagrams of 3-dimensional mathematical model for blast furnace<sup>9)</sup>

Table 1 Reactions considered in mathematical blast furnace model<sup>9)</sup>

No.	Reactions
(4)	$3\text{Fe}_2\text{O}_3(\text{s}) + \text{CO}(\text{g}) = 2\text{Fe}_3\text{O}_4(\text{s}) + \text{CO}_2(\text{g})$
(5)	$\text{Fe}_3\text{O}_4(\text{s}) + \text{CO}(\text{g}) = 3\text{FeO}(\text{s}) + \text{CO}_2(\text{g})$
(6)	$\text{FeO}(\text{s}) + \text{CO}(\text{g}) = \text{Fe}(\text{s}) + \text{CO}_2(\text{g})$
(7)	$3\text{Fe}_2\text{O}_3(\text{s}) + \text{H}_2(\text{g}) = 2\text{Fe}_3\text{O}_4(\text{s}) + \text{H}_2\text{O}(\text{g})$
(8)	$\text{Fe}_3\text{O}_4(\text{s}) + \text{H}_2(\text{g}) = \text{FeO}(\text{s}) + \text{H}_2\text{O}(\text{g})$
(9)	$\text{FeO}(\text{s}) + \text{H}_2(\text{g}) = \text{Fe}(\text{s}) + \text{H}_2\text{O}(\text{g})$
(10)	$\text{C}(\text{s}) + \text{CO}_2(\text{g}) = 2\text{CO}(\text{g})$
(11)	$\text{C}(\text{s}) + \text{H}_2\text{O}(\text{g}) = \text{CO}(\text{g}) + \text{H}_2(\text{g})$
(12)	$\text{FeO}(\text{l}) + \text{C}(\text{s}) = \text{Fe}(\text{l}) + \text{CO}(\text{g})$
(13)	$\text{C}(\text{s}) = \underline{\text{C}}$
(14)	$\text{H}_2\text{O}(\text{g}) + \text{CO}(\text{g}) = \text{H}_2(\text{g}) + \text{CO}_2(\text{g})$
(15)	$\text{SiO}_2(\text{l}) + \text{C}(\text{s}) = \text{SiO}(\text{g}) + \text{CO}(\text{g})$
(16)	$\text{SiO}_2(\text{s}) + \text{C}(\text{s}) = \text{SiO}(\text{g}) + \text{CO}(\text{g})$
(17)	$\text{SiO}_2(\text{s}) + 3\text{C}(\text{s}) = \text{SiC}(\text{s}) + 2\text{CO}(\text{g})$
(18)	$\text{SiO}(\text{g}) + \underline{\text{C}} = \underline{\text{Si}} + \text{CO}(\text{g})$
(19)	$\text{Fe}(\text{s}) = \text{Fe}(\text{l})$
(20)	$\text{FeO}(\text{s}) = \text{FeO}(\text{l})$

Case D are the same as in Case C, high reducibility sinter was used in Case D. Sinter reducibility was changed by switching between the sinters from two sintering machines at Nippon Steel. The reduction index specified in JIS M 8713 (hereinafter abbreviated as JIS-RI) was adopted as an index of sinter reducibility. This is because JIS-RI is currently the only common index that can be used when the sinter reducibility is discussed by ironmaking researchers in Japan. It is under discussion whether JIS-RI is still an appropriate evaluation index for sinter reducibility in a high-hydrogen atmosphere because JIS-RI is measured in a 60% CO-40% N<sub>2</sub> atmo-

Table 2 Operation conditions and predicted reduction ratio of carbon consumption in experimental blast furnace

Case	5th campaign				6th campaign			
	A	B	C	D	A-2	E	C-2	F
COG (Nm <sup>3</sup> /h)	0	119	119	119	0	0	119	0
H <sub>2</sub> (Nm <sup>3</sup> /h)	0	0	170	170	0	143	170	310
Total H <sub>2</sub> input (Nm <sup>3</sup> /t-HM)	53	154	276	277	61	159	276	277
Blast volume (Nm <sup>3</sup> /h)	1589	1188	852	822	1699	1408	904	975
Blast temp. (°C)	1000	1000	1000	1000	1000	1000	1000	1000
O <sub>2</sub> (Nm <sup>3</sup> /h)	94	182	252	252	104	154	259	229
O <sub>2</sub> enrichment (%)	4.4	10.5	18.0	18.5	4.4	9.0	20.0	16.8
Flame temp. (°C)	2098	2101	2096	2091	2086	2094	2091	2091
Reducibility index of sinter (JIS-RI) (%)	64	64	64	68	64	64	64	64
Productivity (t/d)	34	34	34	34	34	34	34	34
Reduction ratio of C emission (%)	0	3.0	8.0	9.0	0.0	5.7	10.7	12.0

sphere at 900°C.

4.2.2 Test operation method

At each test operation, when the hearth brick temperature became constant, it was judged that the operation had reached a steady state. This means that the operation of the experimental blast furnace was continued under the conditions in Case A until the rising rate of the hearth brick temperature decreased and became almost constant. It took 10 days for the hearth brick temperature to become constant, and therefore the experimental blast furnace was judged as having reached a steady state. After the experimental blast furnace reached the steady state, the temperature and gas composition in the furnace were measured. When the scheduled measurements were finished, the operation condition was switched to the next case immediately. The experimental blast furnace was operated under that condition for 2 days in order for it to stabilize. After the status of the experimental blast furnace was judged as stable, the temperature and gas composition in the furnace were measured, and then the operation condition was changed to the next one. This cycle was repeated. As soon as all the test cases were completed, the atmosphere in the furnace was replaced with N<sub>2</sub> and the furnace was left to cool for about one month.

4.2.3 Measurement items

The sinter reducibility is one of the operating factors. It was measured every day during the operation of the experimental blast furnace. The pig iron temperature and the pig iron and slag compositions were measured at every tap so that the blowing and charging conditions were fine-tuned accordingly. After the actual operation conditions were adjusted to the designed operation conditions as described above and were confirmed to be stabilized, the furnace temperature and gas composition were measured with the vertical probe and the horizontal probes installed in three stages in the height direction of the furnace.

4.2.4 Evaluation method

After the campaign was finished, data of a stable 24 h period in each operation condition, where the furnace was judged to have operated stably with an almost constant blast rate, were extracted. The actual results during those periods were averaged and the mass and heat balances were calculated accordingly. The specific carbon consumption rate in each case was calculated from the balance calculation results and compared with the base specific carbon consumption rate in Case A. The reduction rate of carbon consumption was then calculated.

5. Experimental Results

5.1 Operation outline

The transitions in the operating conditions of the experimental blast furnace in the sixth campaign are shown in Fig. 5 as an example. Although pure H<sub>2</sub> gas was injected into the experimental blast furnace at an unprecedented rate in the world, it was continuously operated almost stably for 32 days. Also it was confirmed that when the hydrogen input increased, the hydrogen reduction ratio increased and the direct reduction ratio decreased.

5.2 Gas concentration distribution in the radial direction

The CO and H<sub>2</sub> concentration distributions in the cross-sectional direction of the experimental blast furnace were measured in three stages in the height direction. The measurement results are shown together with the simulation results in Fig. 6. The calculation results almost agreed with the actual results at the respective heights.

5.3 Changes in gas concentrations in the height direction

Figure 7 shows the changes in the CO and H<sub>2</sub> concentrations measured with the vertical probe in the height direction of the experimental blast furnace. The CO and H<sub>2</sub> concentrations in the radial meshes calculated by the three-dimensional mathematical blast furnace model in the height direction of the experimental blast furnace

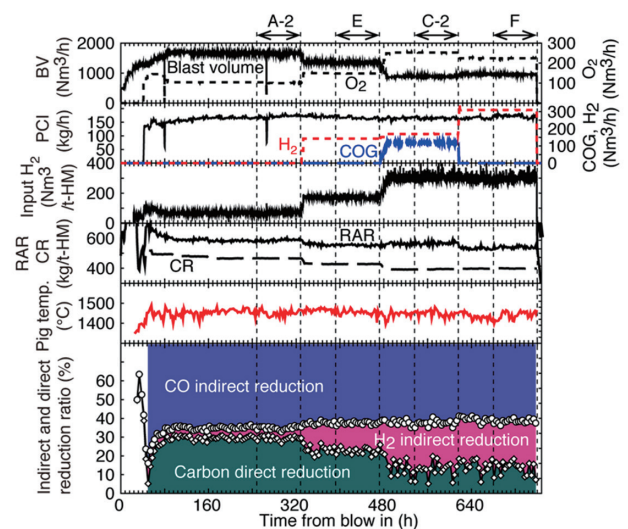


Fig. 5 Operation results of experimental blast furnace (6th campaign)

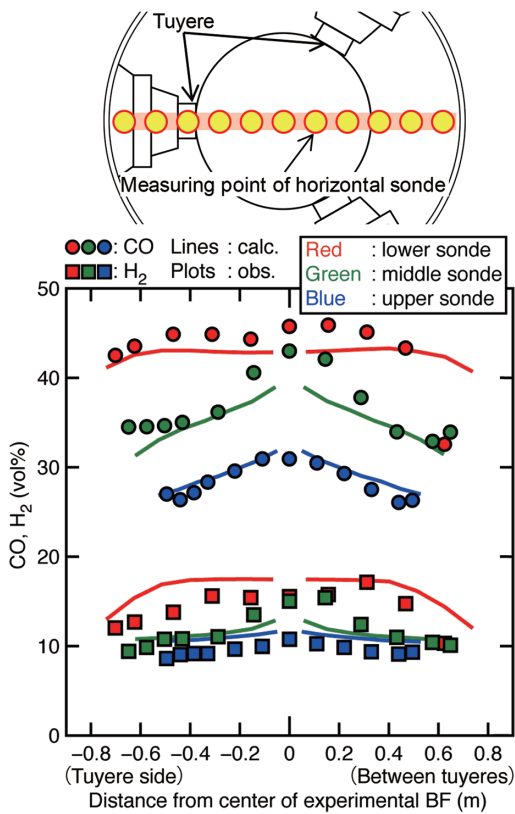


Fig. 6 Example of comparison of observed CO and H<sub>2</sub> concentration distributions by horizontal sondes with calculated ones (Case C)

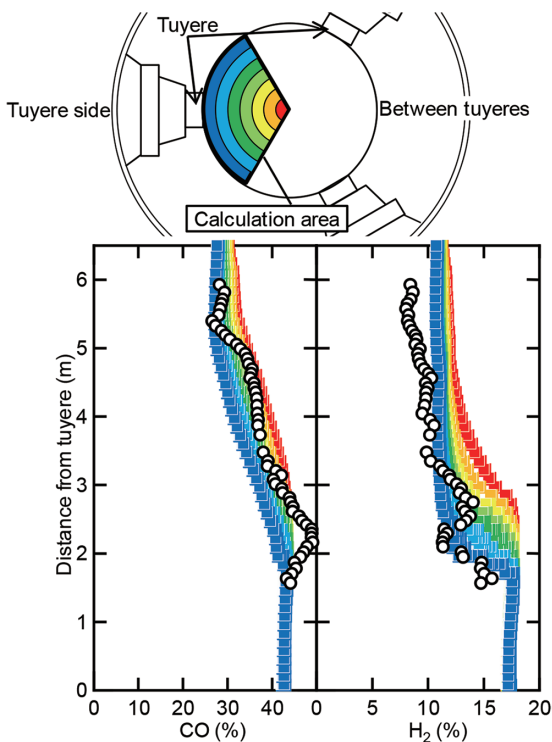


Fig. 7 Example of comparison of observed transitions of CO and H<sub>2</sub> concentrations by vertical sonde with calculated ones (Case C)

are also shown in Fig. 7. The vertical probe descends as the burden descends but does not necessarily move vertically. Moreover, the vertical probe measures the CO and H<sub>2</sub> concentrations at single points. However, the measurement results are practically contained in the bands of the calculation results so that the calculation results are judged to mostly agree with the measured one.

**5.4 Indirect reduction ratio and direct reduction ratio**

Figure 8 compares the CO reduction ratio, H<sub>2</sub> reduction ratio, and direct reduction ratio obtained from the calculation of the mass and heat balances.

The average value of the differences in the direct reduction ratio, CO reduction ratio, and H<sub>2</sub> reduction ratio in Cases A and A-2 was 0.8%. The average difference between Cases C and C-2 was 0.7%. It can thus be judged that the reproducibility is very good. The average difference was slightly larger at 1.7% between Cases B and E and at 0.9% between Cases C and F. The reason is that the CO reduction ratio dropped 2.5% in Case E as compared with Case B and 1.3% in Case F as compared with Case C. This is probably because CO derived from COG decreased as COG injection was replaced with pure hydrogen injection.

The relationship between the total hydrogen input rate and the hydrogen reduction ratio in the 5th and 6th campaigns is shown together with the relationship in the 2nd to 4th campaigns<sup>13)</sup> in Fig. 9. The straight solid line through the plots in this figure is determined by the least squares method using the data observed in the 2nd to 4th campaigns. The operation results of the 5th and 6th campaigns are plotted on the extension line of the solid line obtained by the least squares method.

**5.5 Specific carbon consumption reduction rate**

The relationship between the total hydrogen input rate and the specific carbon consumption reduction rate is shown in Fig. 10. The results of simulation by the three-dimensional mathematical blast furnace model are also shown in Fig. 10. As Fig. 10 shows, the simulation results agreed with the actual results. The total hydrogen input rate being the same, the specific carbon consumption reduction rate increased in the order of COG, COG + H<sub>2</sub>, and pure H<sub>2</sub>. The specific carbon consumption reduction rate increased only 0.5% when high-reducibility sinter was used. It seems that the operation disturbances affected this result, so the influence of the sinter reducibility on the carbon consumption reduction remains a matter for future research.

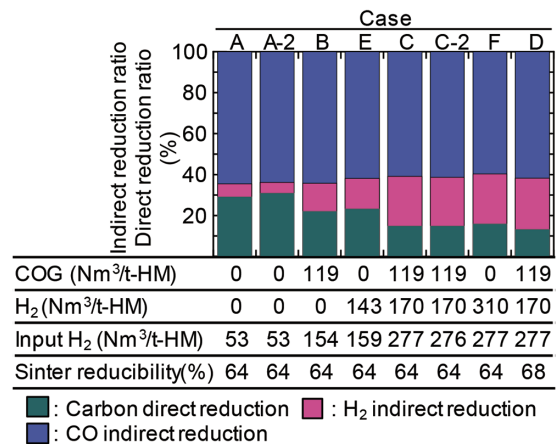


Fig. 8 Comparison of relationship between total input H<sub>2</sub> with indirect reductions and direct reduction

Incidentally, there are two simulation results for the COG + H<sub>2</sub> injection operation. The simulation results near the 8% specific carbon consumption reduction rate are the results predicted by using the parameters up to the 4th campaign<sup>13)</sup>. The maximum total hydrogen input rate in the 4th campaign was 210 Nm<sup>3</sup>/t-HM. The operation of the experimental blast furnace with a total hydrogen input rate of 277 Nm<sup>3</sup>/t-HM was predicted by using the parameters capable of reproducing the operation results up to the total hydrogen input rate of 210 Nm<sup>3</sup>/t-HM. The specific carbon consumption reduction rate was estimated at a maximum of 8%. When the experimental blast furnace was operated under the calculated conditions, the specific carbon consumption rate of 8% was achieved as expected. The parameters were re-tuned by using the operation results of the

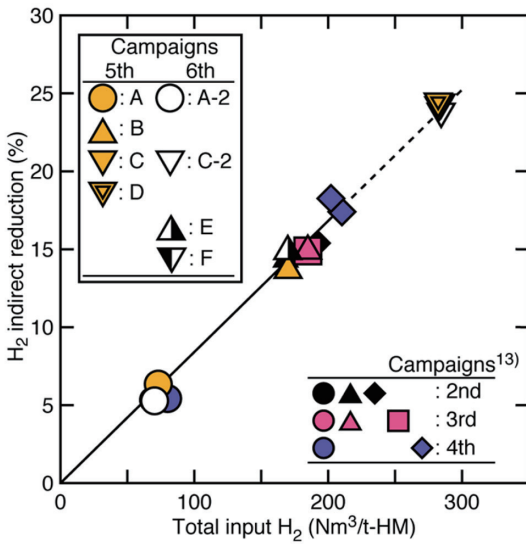


Fig. 9 Relationship between total input H<sub>2</sub> with H<sub>2</sub> indirect reductions

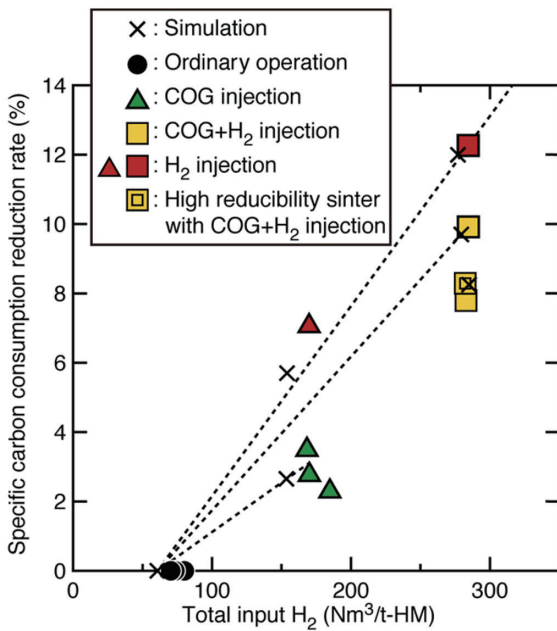


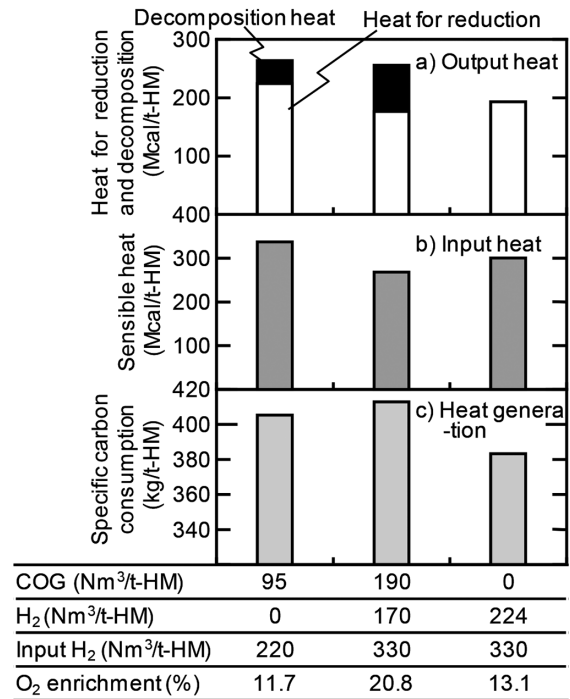
Fig. 10 Relationship between total input H<sub>2</sub> with specific carbon consumption reduction rate

experimental blast furnace with the total hydrogen input rate of 277 Nm<sup>3</sup>/t-HM in the 5th campaign. The operation of the furnace was simulated again with the total hydrogen input rate of 277 Nm<sup>3</sup>/t-HM. As a result, a blast rate-oxygen rate combination at which the specific carbon consumption reduction rate became 10% was found. When the furnace was operated under those conditions in the 6th campaign, the specific carbon consumption reduction rate of 10% was obtained. This is the reason why there are two sets of simulation results and why there are some differences between Cases A and A-2 and between Cases C and C-2 as shown in Table 2. The prediction results of the specific carbon consumption reduction rate during the operation of the experimental blast furnace with pure H<sub>2</sub> gas injection were those conducted by using the re-tuned parameters. The calculation results agree very well with the actual results. The tuning accuracy can thus be judged to have improved. It was demonstrated by the simulation and operation of the experimental blast furnace that the specific carbon consumption reduction rate was 12% when the total hydrogen input rate was 277 Nm<sup>3</sup>/t-HM.

6. Discussion

It was demonstrated by the simulation and operation of the experimental blast furnace that the specific carbon consumption reduction rate varies with the type of gas injected through the tuyeres when the total hydrogen input rate is the same. To investigate the reason for this situation, the heat balance calculated by the three-dimensional mathematical blast furnace model was compared for the injection of COG alone, the injection of both COG and H<sub>2</sub>, and the injection of H<sub>2</sub> alone. The results are shown in Fig. 11.

First of all, the effect of the COG injection rate is described. The heat output of the experimental blast furnace is shown in Fig. 11 a). As the COG injection rate increases, the heat required for reduction



\*Flame temperatures and productivities are constant.

Fig. 11 Comparison of effects of reductant gas types on heat input and output of blast furnace and specific carbon consumption

decreases. This is because the direct reduction ratio decreases. The increase in the COG injection rate also increases the heat of decomposition. As already described, the tests were conducted at a constant flame temperature, pig iron production rate, and pig iron temperature. Gaseous reductants are injected at room temperature. When the injection rate of a gaseous reductant is increased, the oxygen rate is increased to keep the flame temperature constant. At the same time, the blast rate is decreased to satisfy the requirement to keep the pig iron production rate constant. The decrease in the blast rate decreases the amount of N<sub>2</sub> blown into the furnace or specifically the input of sensible heat into the furnace (Fig. 11 b)). As a result, the increase in the COG injection rate increases the specific carbon consumption rate (Fig. 11 c)).

On the other hand, when H<sub>2</sub> is injected alone, the heat of decomposition is not required. At the same total hydrogen input rate, therefore, the injection of H<sub>2</sub> alone can decrease the oxygen enrichment ratio. That is, because it is not necessary to decrease the blast rate, the sensible heat of blown air can be increased. It was thus clarified that the injection of H<sub>2</sub> alone can further decrease the specific carbon consumption rate.

From this result, it is concluded that the injection of H<sub>2</sub> alone is necessary to reduce the CO<sub>2</sub> emissions in this development work in the future. However, hydrogen that can be produced without CO<sub>2</sub> emissions, or green hydrogen, is difficult to obtain. These development activities will be continued in the future so that green hydrogen can be used as soon as it becomes available, but at the same time, the early commercialization of green hydrogen production technology is also necessary.

## 7. Conclusions

Using a three-dimensional mathematical blast furnace model, the effect on CO<sub>2</sub> emissions of injecting hydrogen containing gaseous reductants into blast furnaces was simulated. Based on the simulation results, demonstration tests with a 12 m<sup>3</sup> experimental blast furnace were conducted and the following findings were obtained:

- (1) It was confirmed that CO<sub>2</sub> emissions from the experimental blast furnace could be reduced by 12% when the total hydrogen input rate was 277 Nm<sup>3</sup>/t-HM. This result was demonstrated by continuously operating the experimental blast furnace for 32 days.
- (2) A positive correlation was observed between the hydrogen input and the hydrogen reduction ratio.
- (3) The effect of reducing CO<sub>2</sub> emissions varies with the type of gas injected when the total hydrogen input to the blast furnace

is the same. It was clarified by simulation that the CO<sub>2</sub> emission reduction was affected by the heat of decomposition of the gaseous reductant and by the oxygen injection rate.

## Acknowledgements

The results of this study were obtained as the results of the project entitled “Environmentally Friendly Process Technology Development (COURSE50)” and commissioned by the New Energy and Industrial Technology Development Organization (NEDO). We would like to thank the NEDO.

We would also like to express our deep gratitude to the management and operational personnel for their cooperation in the completion of the test operations and to all persons in and out of Nippon Steel and affiliated with the COURSE50 project. We would also like to express our sincere gratitude to Mr. Ryota Sugitani of Hamada Heavy Industries Ltd. for his efforts in the data analysis of the experimental blast furnace from its hot test operation to the 5th campaign.

## References

- 1) For example, United Nations: The Paris Agreement, <https://unfccc.int/process-and-meetings/the-paris-agreement/what-is-the-paris-agreement>, (accessed 2020-10-7)
- 2) Ariyama, T.: Tetsu-to-Hagané. 105, 567 (2019)
- 3) ThyssenKrupp: Press Release, <https://www.thyssenkrupp.com/en/newsroom/press-releases/world-first-in-duisburg-as-nrw-economics-minister-pinkwart-launches-tests-at-thyssenkrupp-into-blast-furnace-use-of-hydrogen-17280.html>, (accessed 2020-10-8)
- 4) BAOWU: Press Release, [http://www.bygt.com.cn/nzcms\\_show\\_news.asp?id=6558](http://www.bygt.com.cn/nzcms_show_news.asp?id=6558), (accessed 2020-10-7)
- 5) Takahashi, K., Nouchi, T., Sato, M., Ariyama, T.: Tetsu-to-Hagané. 102, 365 (2016)
- 6) Kawashiri, Y., Nouchi, T., Matsuno, H.: Tetsu-to-Hagané. 104, 467 (2018)
- 7) For example, The Japan Iron and Steel Federation: <https://www.jisf.or.jp/course50/outline/>, (accessed 2020-10-7)
- 8) NEDO: Press Release, [https://www.nedo.go.jp/news/press/AA5\\_100769.html](https://www.nedo.go.jp/news/press/AA5_100769.html), (accessed 2020-10-7)
- 9) Takatani, K., Inada, T., Ujisawa, U.: ISIJ Int. 39, 15 (1999)
- 10) Nishioka, K., Orimoto, T., Sakai, H.: CAMP-ISIJ. 28 (2), 613 (2015)
- 11) Tonomura, S., Araki, K., Hase, K., Ujisawa, Y., Nishioka, K., Ishiwata, N.: 8th International Congress on Science and Technology of Ironmaking (ICSTI 2018), Vienna, 2018
- 12) Kakiuchi, K., Ujisawa, Y., Sunahara, K., Tomisaki, S., Demi, H., Sasaki, M.: 8th International Congress on Science and Technology of Ironmaking (ICSTI 2018), Vienna, 2018
- 13) Nakano, K., Ujisawa, Y., Kakiuchi, K., Nishioka, K., Sunahara, K., Matsuura, Y., Yokoyama, H., Sakai, H.: 8th International Congress on Science and Technology of Ironmaking (ICSTI 2018), Vienna, 2018

**NIPPON STEEL TECHNICAL REPORT No. 127 JANUARY 2022**



Chikashi KAMIJO  
Chief Manager, Ph.D. (Engineering)  
Experimental Blast Furnace Project Div.  
Process Research Laboratories  
1 Kimitsu, Kimitsu City, Chiba Pref. 299-1141



Yoshinori MATSUKURA  
Chief Manager  
Experimental Blast Furnace Project Div.  
Process Research Laboratories



Hirokazu YOKOYAMA  
Senior Manager  
Experimental Blast Furnace Project Div.  
Process Research Laboratories



Kohei SUNAHARA  
Senior Manager, Head of Dept., Ph.D. (Environmental studies)  
Research Plant Dept.  
Experimental Blast Furnace Project Div.  
Process Research Laboratories



Kazumoto KAKIUCHI  
General Manager, Head of Div.  
Experimental Blast Furnace Project Div.  
Process Research Laboratories  
(Currently General Manager, Decarbonization & DX  
Planning Section, Plant & Machinery Sector, Nippon  
Steel Engineering Co., Ltd.)



Kaoru NAKANO  
General Manager, Head of Dept.  
Blast Furnace & Decarbonization Research Dept.  
Ironmaking Research Lab.  
Process Research Laboratories



Hiroshi SAKAI  
Senior Researcher  
Ironmaking Research Lab.  
Process Research Laboratories